Applied Environmental Research
- RESEARCH FOR SUSTAINABLE PLANET -

Research Article

Geospatial Modelling of Flood Susceptibility of the Calabar City, Cross River State, Nigeria

Joel Efiong[1,*], Eme Joel Efiong[2], Oluyemi A. Akintoye[1], Ebin Okah Inah[3], Obianuju Emmanuella Awan[1], Francis Effime Ogban[4]

[1] *Department of Environmental Management, University of Calabar, Calabar, Nigeria*
[2] *Department of Accounting, University of Calabar, Calabar, Nigeria*
[3] *Department of Geography and Environmental Science, University of Calabar, Calabar, Nigeria*
[4] *Department of Urban and Regional Planning, University of Cross River State, Nigeria*

*Correspondence Email: joelefiong@unical.edu.ng

Abstract

Flooding remains a major environmental problem in many parts of the world including Nigeria, causing untold losses. This study modelled the flood susceptibility of Calabar Metropolis using frequency ratio and geographical information system (GIS). Direct field observation and key informant approaches were used to obtain 127 previous and current flood locations in the study area from which a database of historical flood occurrence was developed. Using the geostatistical analyst tool within a geographical information environment the flood locations were split into two parts in the ratio of 70:30 percent for the training and testing processes, respectively. Eight flood conditioning factors (elevation, slope, aspect, curvature topographic position index, topographic wetness index, land cover and normalized difference vegetation index) were extracted from SRTM-30m DEM and Landsat 8 data accordingly and used in the geospatial analysis of flood occurrence within the GIS. The frequency ratio model was then developed using the training dataset. The final product was the flood susceptibility map of the study area. The results revealed that 9.3 percent of the study area was considered to have very high flood susceptibility, 19.97 percent was classified as high flood susceptibility while 31.79 percent was under moderate risk area. About 39 percent of the study area was classified at least under low flood susceptibility. The order of contribution of the conditioning factors to the model were topographic position index (TPI), elevation, normalized difference vegetation index (NDVI), land cover, curvature, aspect, slope, and topographic wetness index (TWI). The validation of the model using the receiver operating characteristics (ROC) curve returned an AUC value of 74.81 percent. Hence, the result was acceptable for the prediction of flood locations in the study area. The findings would assist urban planners, environmental managers, risk reduction and management agencies, land developers, policy makers, and indeed the general public.

ARTICLE HISTORY
Received: 7 May 2024
Accepted: 4 Sep. 2024
Published: 23 Sep. 2024

KEYWORDS
Frequency ratio;
Flood susceptibility;
Mapping;
Calabar;
Nigeria;
Spatial analysis

Introduction

Globally and on a yearly basis, natural disasters including droughts, earthquakes, landslides, and floods have continued to cause untold deaths and property destruction. However, flood has been adjudged as the most destructive of all natural disasters due to its wide-spread impacts whenever it occurs [1]. Flood occurrence could hinder a lot of activities in the environment such as transportation systems, agriculture, socio-cultural and general human life. Flood is said to account for about

40 percent of all losses due to natural disasters [2–3]. Several factors account for impact of flood in any location. They include topography, land use pattern, population growth, forest removal, poor infrastructure, low residence, social mentality and so on [4–7].

There are several types of floods which include river flood, coastal flood, storm surge, inland flood and flash flood. When water levels rise over the top of river banks because of excessive rain over the same area for an extended period, it is termed river flood. A coastal flood occurs due to the inundation of land areas along the coast. Storm surge results from the abnormal rise in water levels, over and above regular astronomical tides in coastal areas. This is often caused by forces generated from severe storms, wind, waves, and low atmospheric pressure. Inland flooding arises when moderate precipitation accumulates over a period or due to dam failure. Heavy and excessive rainfall over a short period of time (generally less than 6 hours) often leads to flash floods. Flash flood can also occur due to dam failure. It has been stated that almost one-third of the global land area is vulnerable to the risk of flooding [8].

Flooding has become a recurrent decimal in many parts of Nigeria with its attendant negative impact [9-13]. In 2012, flood affected 30 states in Nigeria killing 363 people while over 2.1 million others were displaced, with an estimated cost of 9.6 billion USD on the Nigerian economy. The 2012 flood was the worst in 40 years [13] affecting over 7 million people [15]. The total damages and losses due to the flood were estimated at 2.6 trillion [16]. The National Emergency Management Agency (NEMA) noted that 30 of Nigeria's 36 states were affected by the 2012 flood. Be that as it may, the 2022 flood experience in Nigeria is argued to be worse than the 2012 flood.

In recent years, Calabar City, like many other cities in Nigeria, has witnessed an increase in flood events, leading to significant economic losses, displacement of populations, and environmental degradation (Figure 1). The Cross River State Emergency Management Agency reported that no fewer than 15 persons died between the months of August and September 2017 due to flooding along Target, Murray, Goldie, Ebito and the lower parts of Nelson Mandela streets in Calabar [17]. The recurrent nature of these floods underscore the vulnerability of the region to such natural disasters, exacerbated by a combination of geographical, climatic, and human factors. Despite the critical need to understand and mitigate flood risks, there remains a significant gap in comprehensive flood risk management strategies that are informed by reliable and localized flood susceptibility models.

Current approaches to flood management in Calabar City are primarily reactive rather than proactive, with emergency responses that focus on post-event relief efforts. Such approaches are not only costly but also insufficient in reducing the long-term impacts of flooding on the community and infrastructure [5, 11–12]. Moreover, the lack of precise, data-driven models to predict flood-susceptible areas hampers effective planning and implementation of mitigation measures. Traditional flood risk assessments in the area have often overlooked the complex interplay of various factors that contribute to flood susceptibility, such as topography, land cover, drainage patterns, and changing climatic conditions [11, 18–19]

The accurate prediction of flood susceptibility of a particular region has become an important step in land management and policy formulation for the mitigation of flood risk [20]. Hence, flood susceptibility modelling has become the beginning stage of flood management all over the world [3, 21–24]. To achieve this, researchers use robust approaches to provide maps with precise and accurate results. Such map outputs often help in proposing flood management plans [3, 22].

(a) (b) (c)

Figure 1 Impacts of flooding in Calabar (a) flooding along Target by Goldie Street in Calabar (Lat. 4°57′17″N; Lon. 8°19′41″E. Date: 22/09/2022), (b) flood pulled down a fence along Ebito Street in Calabar (Lat. 4°57′07″N, Lon. 8°19′38″E. Date: 17/06/2023), and (c) flood water on Target Road (Lat. 4°57′16″N; Lon. 8°19′39″E: 14/07/2023).

Flood susceptibility modelling involves the use of various data and techniques to identify areas prone to flooding. The approach analyses conditioning factors such as topography (elevation, slope, aspect, etc.), geology, land use and land cover (urbanization, vegetation), precipitation patterns, rainfall amount, and their relationships with flood locations. When these factors are combined using either statistical, machine learning, or even physical modelling approaches, flood susceptibility models can be developed. These models have the capacity to predict the likelihood of flooding in the various segments of a study area. The information can then be used for several purposes including flood risk assessment and mapping, urban planning and development, emergency preparedness and response, environmental management, and conservation.

Literature is replete with common approaches and techniques used in flood susceptibility modelling. They include logistic regression [25–26], decision trees [27–28], random forest [29-30], support vector machines (SVM) [31–32], artificial neural networks (ANN) [33–34], frequency ratio [35–42] and analytical hierarchy process (AHP) [43–47]. The use of any of these techniques depend on the interest of the study. Meanwhile the frequency ratio, which is a bivariate statistical method, has been shown to offer an excellent quantitative approach to evaluate the impact of each contributing factor on flood occurrences, thereby enabling targeted interventions. Hence, the reason for its adoption in the present study.

The absence of such models has posed a serious barrier to the effective allocation of resources for flood risk reduction, land-use planning, and urban development policies in the study area. Without a detailed understanding of flood dynamics and susceptibility patterns within Calabar City, efforts to minimize the impact of floods and enhance community resilience remain hampered. Consequently, there is an urgent need for an integrated flood susceptibility model that can guide decision-makers in prioritizing areas for intervention, enhancing early warning systems, and implementing sustainable flood management practices.

In view of the above, this study; 1. examined the nature of the various flood conditioning factors in Calabar City; 2. investigated the influence of the various conditioning factors on flood susceptibility of Calabar City; 3. developed a robust flood susceptibility model for the study area; 4. validated the developed model in 3 above. The output can significantly contribute to the reduction of flood risks and the promotion of a safer, more resilient urban environment in Calabar City, Cross River State, Nigeria. This work is therefore significant to urban planners, environmental managers, risk reduction and management agencies (e.g. The National Emergency Management Agency), land developers, policy makers, and indeed the general public.

Materials and methods

1) Study area: Calabar

The geographical location of Calabar is shown in Figure 2. It is a coastal city in Nigeria and the capital of Cross River State. Calabar is sandwiched by two great rivers: the Calabar River and the Great Kwa River. The two rivers meet at the Cross River estuary which empties into the Atlantic Ocean. The city sits on a landmass of approximately 137 km^2.

Major geomorphic features which could have significant controls on flooding in the city include:

1. The bold Marina escarpment or cuesta, which occupies the western flank of the city fronting the Calabar River meander loop and runs from Calcemco (Larfarge) Beach through Nsidung Beach.

2. The two main ridges running parallel to each other, one to the west and the other to the east. The main ridge to the west runs from Ikot Ekpo/Tinapa Area in the northern part of the city to Mbukpa in the south and covers about 40 percent of the entire city [4]. The second ridge runs almost along the well-known Eastern Highway and rises only to about 60 m above sea level. Runoff from both ridges empties into the geosyncline or depression which cuts across the city.

3. The geosyncline which separates the two ridges and runs in the north-south direction. This depression originates from the New Secretariat axis and runs through Big Qua Town, Otop Abasi Barracks, Bogobiri, Target, Murray and Palm streets to the University of Cross River State Staff Quarters. This geosyncline is the lowest portion of Calabar City and constitutes the greatest drainage problem in the city. Locations along this depression always experience periodic flooding [4].

Rainfall in the study area is continuous throughout the year. It has a double-maxima rainfall regime with peaks in June/July and September/October. The average annual rainfall is above 2,000 mm. Temperature rarely falls below 19°C and averages 27°C all year round [48]. Based on Koppen's climatic classification, the area is described as a tropical rainforest climate. With the above climatic characteristics, the area is considered a humid tropical environment.

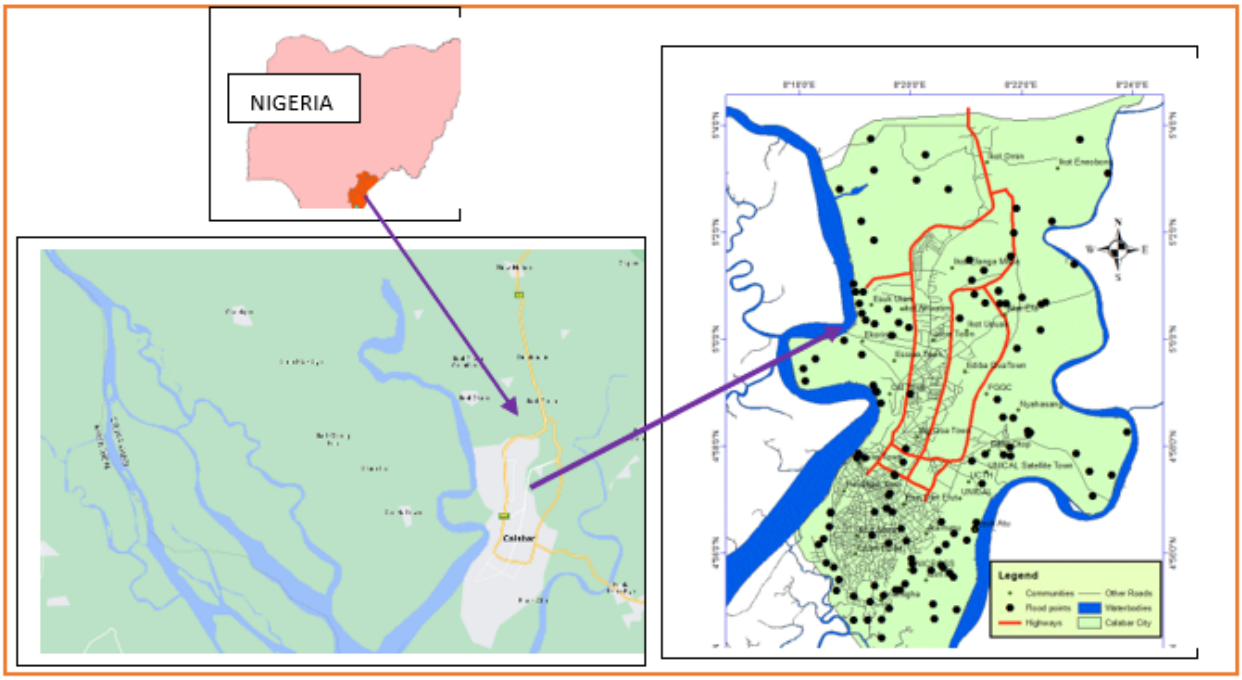

Figure 2 Study area showing historical flood locations.

Most of the original land cover (vegetation) in the study area has been replaced as a result of urban development. There are marginal wetlands on the eastern and southern flanks of the city which are currently under serious threats of urban encroachment. These conditions would certainly have an influence on flooding in the city. Geologically, the study area is situated within the Benin Formation of the Niger Delta Basin. The Formation comprises coarse grained, unconsolidated sands and gravel with minor intercalation of clays of Tertiary age. It lies unconformably on the Nkporo Shales of the Calabar Flank. On top of the sands are the alluvial deposits [49]. This kind of geology could enhance infiltration of water into the soil. However, the area has been seriously modified by urban development with associated high runoff volume.

2) Data collection

Data for the extraction of flood conditioning factors used in the development of flood susceptibility map were collected and extracted from the Shuttle Radar Topography Mission (SRTM)-30 m resolution digital elevation model (DEM) and Landsat 8 satellite imageries via the internet at [50] and [51] respectively. The choice of SRTM DEM was because it offers worldwide coverage of void filled data at a resolution of 1 arc-second (30 m) and provides open distribution which is readily available and at no cost. Moreover, flood susceptibility maps produced using SRTM-30m DEM have been found to be of reasonably good accuracy [38]. Flood conditioning factors such as elevation, slope gradient, aspect, curvatures, topographic position index (TPI) and topographic wetness index (TWI)were extracted from the DEM.

Landsat 8 imagery date was 12th January 2023, a period with the highest chance of obtaining cloud-free imageries of the study area. The land cover map of the study area was produced from the obtained satellite imagery using the supervised classification algorithm. The normalized difference vegetation index (NDVI) was also produced from satellite imagery. A total of 127 flood locations were identified and mapped using historical records from published and unpublished documents and direct field observation from 2012 to 2023 (Supplementary Material 1). Figure 3 presents the flow chart for the methodology that was adopted in the study.

3) Development of flood inventory map

From the 127 flood locations that were identified and mapped, a flood database was created from where a flood inventory (FI) map was developed in the GIS. Seventy (70) percent of flood locations were used to train the model, while the remaining 30 percent were used for testing. The training and testing datasets were statistically determined from the inventory of flood locations in the study area with the use of the geo-statistical analyst tool within the GIS environment.

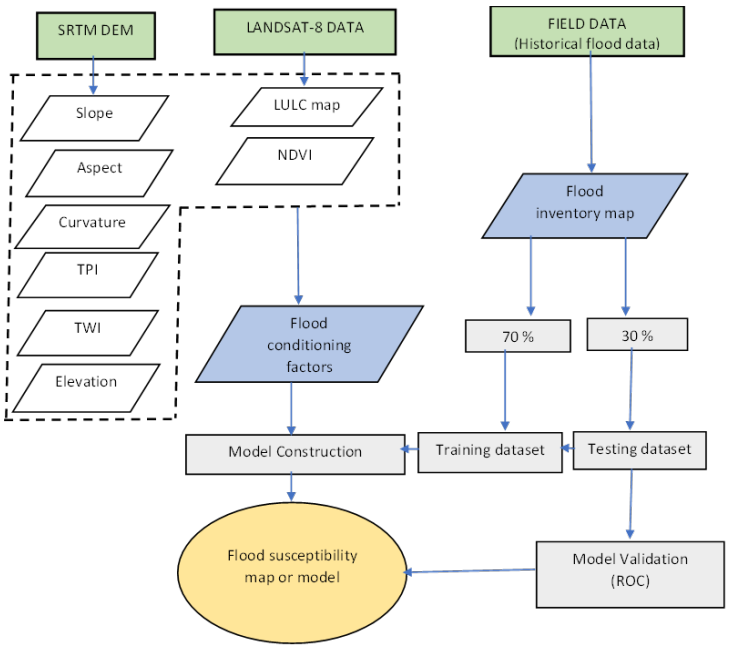

Figure 3 Flow chart of the methodology applied for flood susceptibility analysis.

4) Methods for preparing flood conditioning factors

The development of flood susceptibility model of an area is usually a very complex process, requiring several inputs variables of topographic and hydrologic nature. The selection of flood conditioning factors in a particular region to be included in the model is critical to the validation and accuracy of the susceptibility map [22]. Based on available literature and nature of the study FTPI important and used to model the susceptibility of Calabar in Cross River State of Nigeria to flooding. The factors were elevation, slope, aspect, curvature, TPI, and TWI. Others were land cover and NDVI. These are common conditioning factors used in previous studies [23, 35-39, 44-45]. They were all transformed into raster format with spatial resolution of 30 m. Moreover, the small size of the study area (137 km^2) made it difficult to include other data sets because they could not present any significant variance in their distribution. For instance, data on rainfall distribution, soil and geology were excluded from the study due to the uniform nature of their distribution over the study area.

4.1) Elevation

Elevation in this study was taken simply as the height above or below a fixed reference point of a geographic location. It was obtained from the digital elevation model. Elevation was measured in metres.

4.2) Slope

One of the first derivatives of elevation is slope and was obtained for the purpose of quantifying the variations in elevation over distance. It is an important parameter in hydro-geomorphological studies including flooding and management of flowing water. Slope was calculated based on the elevation of a point and its 8 neighbours. The slope algorithm was taken as Eq. 1 [52].

$$Slope = arctan[\sqrt{x^2 + y^2)}] \quad \text{(Eq. 1)}$$

where x and y are the cell sizes in the x and y directions respectively. Slope generally decreases with the flattening of the terrain and as such has significant effect on water flow. Slope was measured in degrees.

4.3) Aspect

Aspect is another derivative of elevation that affect the directions of water flow, though indirectly. It was determined as the angle between the y-axis and the direction in which the slope is steepest from the clockwise direction [52]. Aspect is usually measured in degrees with values varrying from 0 to 360^o and has direct influence on rainfall intensity, a major contributor to flood episodes. Aspect was obtained using the following Eq. 2 [52].

$$Aspect = \arctan(slope\ in\ x / slope\ in\ y) \quad \text{(Eq. 2)}$$

4.4) Curvature

Curvature is simply described as the "slope of the slope" of a surface [52]. It distingushes the convergent and divergent runoff locations [53]. While the convergent operations relates to negative value regions, the divergent operations goes with the positive. Convergent areas are highly susceptible to flash floodings. Generally, curvature affects the flooding budget and has been used by several scientists to predict areas that are susceptible to future flood occurrence [22]. Curvature was obtained by fitting

a fourth-order polynomial to a 3 x 3 window of a DEM and expressed as Eq. 3 [52].

4.5) Topographic position index (TPI)

Topographic position index (TPI) reflects the difference between the focal cell elevation and the mean elevation of all cells in the neighbourhood of the focal cell [41]. TPI is an effective factor for debris and water flow. Positive TPI values represent areas that are higher than the average of their surroundings (ridges). Negative TPI values represent locations that are lower than their surroundings (valleys). Areas with negative TPI have higher risk of flooding than those with positive TPI [54]. TPI is a dimensionless parameter.

4.6) Topographic wetness index (TWI)

Topographic wetness index (TWI) It reflects the amount of water contained in every pixel size of the study area [52]. Lower TWI represents areas with steepest slope and tend to be ridges or crests present on the landscape. Higher TWI represents areas with increased accumulated runoff potential. TWI for this study was calculated based on the Eq. 4–5 [52].

4.7) Land cover

Land cover describes the materials which are present on the surface such as vegetation, soil-rock, water, and others. The land cover map for the study area was developed from Landsat 8 data using the supervised classifier algorithm within the GIS. The Landsat 8 data was obtained via: [48]. Four bands (2 – 5) were downloaded and then stacked using Erdas Imagine 2014. The bands had the following properties: Band 2 – blue (0.45 – 0.52 μm); band 3 – green (0.53-0.59 μm); band 4 – red (0.64 – 0.67 μm) and band 5 – near-infrared (0.85-0.88 μm). Spatial resolution of the data was 30 m and was acquired on 12th January 2023 having Path/Row no: 188/056. Land cover was measured in terms of areal coverage (m^2).

4.8) Normalized difference vegetation index (NDVI)

The normalized difference vegetation index (NDVI) was used to quantify vegetation greenness and is useful in measuring the difference between vegetation and impermeable surfaces. NDVI was obtained from Landsat 8 data obtained on 12th January 2023. It was calculated using the band ratio method on Landsat 8 OLI data in ArcGIS (Raster calculator) as follow Eq. 6–7 [55].

NDVI is a dimensionless parameter with values varrying from -1 to 1. Generally, low values of NDVI indicate impermeable areas and high values suggest vegetation cover. Specifically, NDVI = -1 to 0 represents water bodies. NDVI = -0.1 to 0.1 represent barren rocks, sand, or snow. NDVI = 0.2 to 0.5 represent shrubs and grasslands or senescing crops. NDVI = 0.6 to 1.0 represents dense vegetation or tropical rainforest [55].

5) Frequency ratio (FR) model

FR was given as the ratio of points in factor class divided by total points to the factor class area divided by total area. FR is expressed mathematically as in Eq. 8 [23].

$$Z = Ax^2y^2 + Bx^2y + Cxy^2 + Dx^2 + Ey^2 + Fxy + Gx + Hy + I \quad \text{(Eq. 3)}$$

where A, B, C, D, E, F, G, H and I are coefficients determined from the surface. Curvature was measured in degrees per metre.

$$\text{TWI} = \ln\frac{\alpha}{\tan\beta+C} \quad \text{(Eq. 4)}$$

$$= \ln\frac{(\alpha+1)*\text{Cell size}}{\tan(\beta*\pi/180)+C} \quad \text{(Eq. 5)}$$

where α is the flow accumulation, β is the slope (in rad) and C (constant term) given as 0.001. TWI is a dimnsionless parameter.

$$\text{NDVI} = \frac{(NIR-R)}{(NIR+R)} \quad \text{(Eq. 6)}$$

$$= \frac{(Band\ 5-Band\ 4)}{(Band\ 5+Band\ 4)} \quad \text{(Eq. 7)}$$

$$FR = \frac{N_i^p/N}{N_i^{lp}/N^l} \quad \text{(Eq. 8)}$$

where N_i^p is the number of pixels in each flood conditioning factor class, N is the number of all pixels in the study area, $N_i^{lp}$is the number of flood locations in each flood conditioning factor class, and N^l is the total number of floods in the study area.

Values of FR greater than 1 indicate a stronger correlation, which means that the percentage of flooding is greater than the region while values less than 1 indicate a weaker correlation [40]. Results of the FR of each class of each conditioning factor were determined as shown in Table 1.

Next, the FR was normalized as the relative frequency (RF) for a range of probability levels (0, 1) using Eq. 9 [22] and the results are on Table 1.

$$RF = \frac{Factor\ class\ FR}{\Sigma\ Factor\ class\ FR} \quad \text{(Eq. 9)}$$

Next, to solve the problem of assigning equal weights to all conditioning variables and to discover the mutual interdependence of flood conditioning factors, a prediction rate (PR) was determined. This was achieved by ranking each flood conditioning factor using the training data set as shown in Eq. 10 [31].

$$PR = (RF_{max} - RF_{min})/(RF_{max} - RF_{\min}) \quad \text{(Eq. 10)}$$

Where $(RF_{max} - RF_{min})_{\min}$ is the minimum value among all computed $RF_{max} - RF_{min}$ values for the conditioning factors.

6) Flood susceptibility map

A flood susceptibility map was developed by calculating and classifying flood susceptibility index (FSI) for Calabar. Using the prediction rates of the individual flood conditioning factors obtained during the training process (Table 1), the FSI was obtained using Eq. 11.

$$FSI = Landcover * b_1 + NDVI * b_2 + Slope * b_3 + Aspect * b_4 + TPI * b_5 - TWI * b_6 + Curvature * b_7 + Elevation * b_8 \quad \text{(Eq. 11)}$$

where $b_1 - b_8$ are the prediction rates associated with each of the conditioning factors. The calculated FSI values were classified, using the Natural breaks (Jenks) method, into five classes: very low, low, moderate, high and very high. Table 2 shows the percentage area coverage of the various classes of the flood susceptibility map.

Table 1 Determination of frequency ratio and prediction rate

Conditioning factor	Class	Class Name/range	Class pixels	% Class pixels (b)	Flooded points	% Flood points (a)	FR=a/b	RF	PR
Land cover	1	Undisturbed forest	35958	23.56	7	7.87	0.33	0.006	1.48
	2	Disturbed forest	13544	8.88	4	4.49	0.51	0.009	
	3	Grassland/open parks	27	0.02	1	1.12	56	0.946	
	4	Cropland	42795	28.04	14	15.73	0.56	0.009	
	5	Built-up	59540	39.01	63	70.79	1.81	0.03	
	6	Water body	744	0.49	0	0	0	0	
NDVI	1	0.02 – 0.11	29944	19.58	65	73.03	3.73	0.695	1.52
	2	0.11 – 0.15	32969	21.56	13	14.67	0.68	0.127	
	3	0.15 – 0.19	32146	21.02	4	4.49	0.21	0.039	
	4	0.19 – 0.22	41949	27.43	3	3.37	0.32	0.059	
	5	0.22 – 0.38	15926	10.41	4	4.49	0.43	0.08	
Slope	1	0 – 2.36	64767	42.36	71	79.78	1.88	0.5	1.09
	2	2.36 – 4.73	49670	32.49	12	13.48	0.41	0.109	
	3	4.73 – 7.93	22145	14.49	6	6.74	0.47	0.125	
	4	7.93 – 12.25	11814	7.73	0	0	0	0	
	5	12.25 – 26.15	4487	2.93	0	0	0	0	
Aspect	1	-1 – 68	29456	19.27	13	14.6	0.76	0.154	1.21
	2	68 – 141	32760	21.43	16	17.98	0.84	0.171	
	3	141 – 212	30730	20.1	24	26.97	1.34	0.273	
	4	212 – 282	31672	20.72	32	35.96	1.74	0.353	
	5	282 – 359	28265	18.49	4	4.49	0.24	0.049	
TPI	1	-3.2	7818	5.11	10	11.24	2.2	0.395	2.89
	2	-0.75	36155	23.65	39	43.82	1.85	0.332	
	3	-0.25 – 0.25	64685	42.31	26	29.21	0.69	0.124	
	4	0.25 – 1.03	36080	23.6	13	14.61	0.62	0.111	
	5	1.03 - 4.47	8145	5.33	1	1.12	0.21	0.038	

Table 1 Determination of frequency ratio and prediction rate (*continued*)

Conditioning factor	Class	Class Name/range	Class pixels	% Class pixels (b)	Flooded points	% Flood points (a)	FR=a/b	RF	PR
TWI	1	4.12 – 6.43	37063	24.24	8	8.99	0.37	0.072	1
	2	6.43 – 7.53	60917	39.85	37	41.57	1.04	0.202	
	3	7.53 – 8.89	32858	21.49	30	33.71	1.57	0.304	
	4	8.89 – 10.60	15657	10.24	10	11.24	1.1	0.214	
	5	10.60 – 16.69	6388	4.18	4	4.49	1.07	0.208	
Curvature	1	-4.4	28839	18.86	12	13.48	0.71	0.281	1.43
	2	-0.23 – 0.19	79103	51.74	68	76.41	1.48	0.585	
	3	0.19 – 3.02	44941	29.4	9	10.11	0.34	0.134	
Elevation	1	<10m	23531	15.39	82	92.14	5.99	0.965	2.56
	2	10 – 30 m	59026	38.61	6	6.74	0.17	0.027	
	3	30 – 50m	33510	21.92	1	1.12	0.05	0.008	
	4	50 – 70m	28538	18.67	0	0	0	0	
	5	70 – 96m	8278	5.41	0	0	0	0	

Note: FR – Frequency ratio; RF – Relative frequency; PR – Prediction rate

Results

1) Nature of the flood conditioning factors

Eight flood conditioning factors (elevation, slope, aspect, curvature, TPI, TWI, land cover and NDVI) were examined in this study and their overlays with flood points are shown in Figure 4.

The results reveal that elevation in the study ranged from 0 to 96 m above sea level (Figure 4a). About 39 percent of the study area has elevation < 30 m above the mean sea level. Of this, 15 percent of the area lies below 10 m above mean sea level. Slope in the study area ranged from 0 and 26.26º (Figure 4b). Curvature for the study area ranged from -4.6 to 3.1 (Figure 6d). The TPI values for Calabar ranged from – 4.20 to 4.48 (Figure 6e) while TWI layer ranged in values from 2.00 to 6.00 (Figure 6f). Six (6) land cover classes were extracted as follows: undisturbed forest, disturbed forest, grassland/open parks, cropland, built-up and water body (Figure 6g) while NDVI in the study area varies between 0.02 and 0.38 (Figure 6h).

2) Influence of conditioning factors on flood susceptibility

Table 1 presents results of the frequency ratio analysis and prediction rates for all the flood conditioning factors that were included in the study. It also shows the distribution of flood points (training data set) over the various classes in each of the factors. An inspection of the table with respect to the distribution of elevation reveals that about 92.14 percent of the flood points occur on elevation of <10 m. Hence most of the flooding in the study area occurred in areas with elevation of <10 m mean sea level. Table 1 also reveals occurrence of 76.41 percent of flood points on near flat surfaces. About 13.48 percent of flood points overlay on concave slopes while the remaining 10.11 per cent were found on convex slopes. For the 5 classes of TW1, 8.99 percent of flood points occured within class 1; 41.57 percent within class 2 and 33.71 percent within class 3. Also, 11.24 percent of flood points were within class 4 while 4.49 percent was within class 5. TPI also exhibited a similar trend like TWI.

On the influence of slope on flood susceptibility, Table 1 reveals that 79.78 percent of the flood points occurred within for slope class 1 (0-2.36°), 13.48 percent occurred within class 2 (2.36-4.73°) while 6.79 percent within slope class 3 (4.73-7.93°). There was no flood occurrence on slope classes 4 (7.93-12.25°) and 5 (12.25 -26.15°). Table 1 again reveals high occurrence of flood points on locations with lower NDVI in the study area. For instance, 73.03 percent of the flood points occurred within NDVI class 1 (0.02-0.11). NDVI class 2 had the second highest occurrence (14.67 percent) of flood points.

Also, there were significant variations in the occurrence of flood across the various land cover classes in the study area. For instance, Table 1 reveals that about 70.79 percent of flood in the study area occurred over built-up surfaces. This accounted for the highest for all land cover types. It was followed by cropland with 15.73 percent while no flood point occurred over waterbody. Further, land cover distribution reveals that 7.83 percent of flooding occurred in undisturbed forest.

Figure 5 presents a summary of the influence of flood conditioning factors on flood susceptibility in Calabar city. Individually, TPI with the prediction rate of 2.89 made the highest contributor to flooding in the study area. This was followed by elevation, NDVI, land cover, curvature, aspect, slope and TWI, in that order.

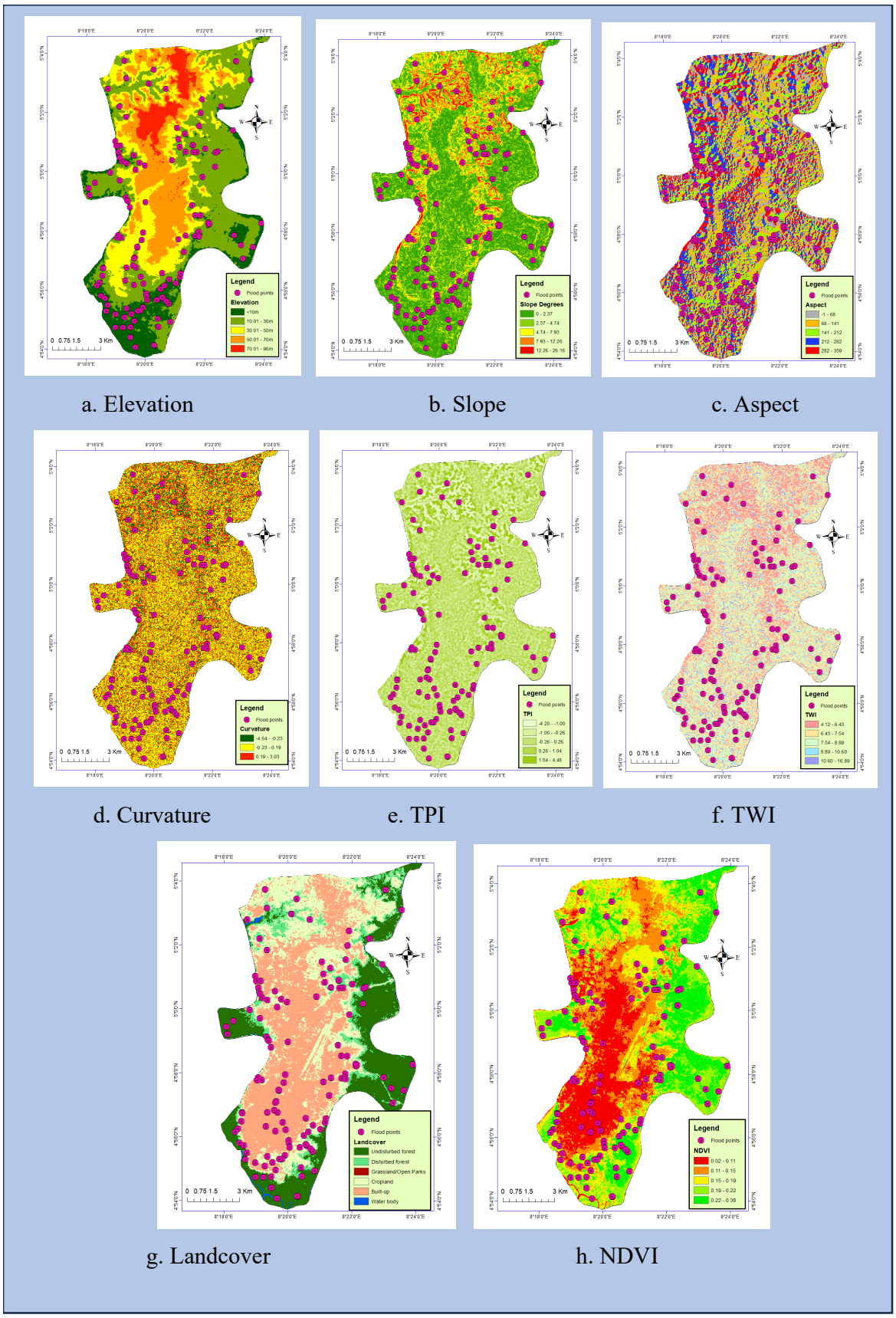

Figure 4 Overlays of flood points on the raster maps of flood conditioning factors.

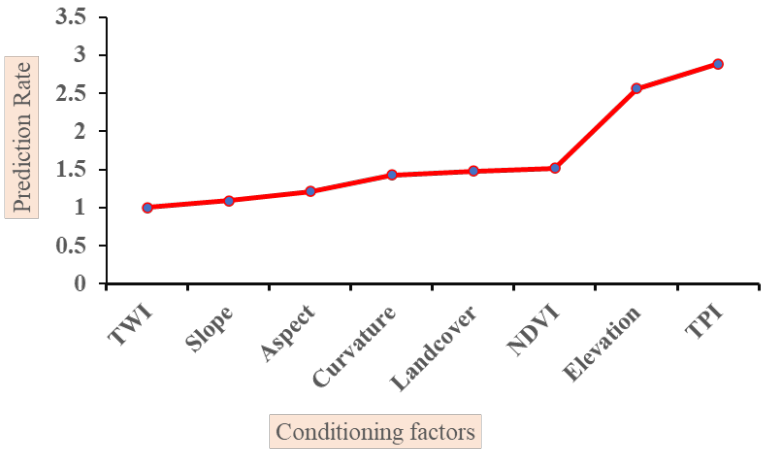

Figure 5 Contributions of conditioning factors to flood susceptibility in Calabar.

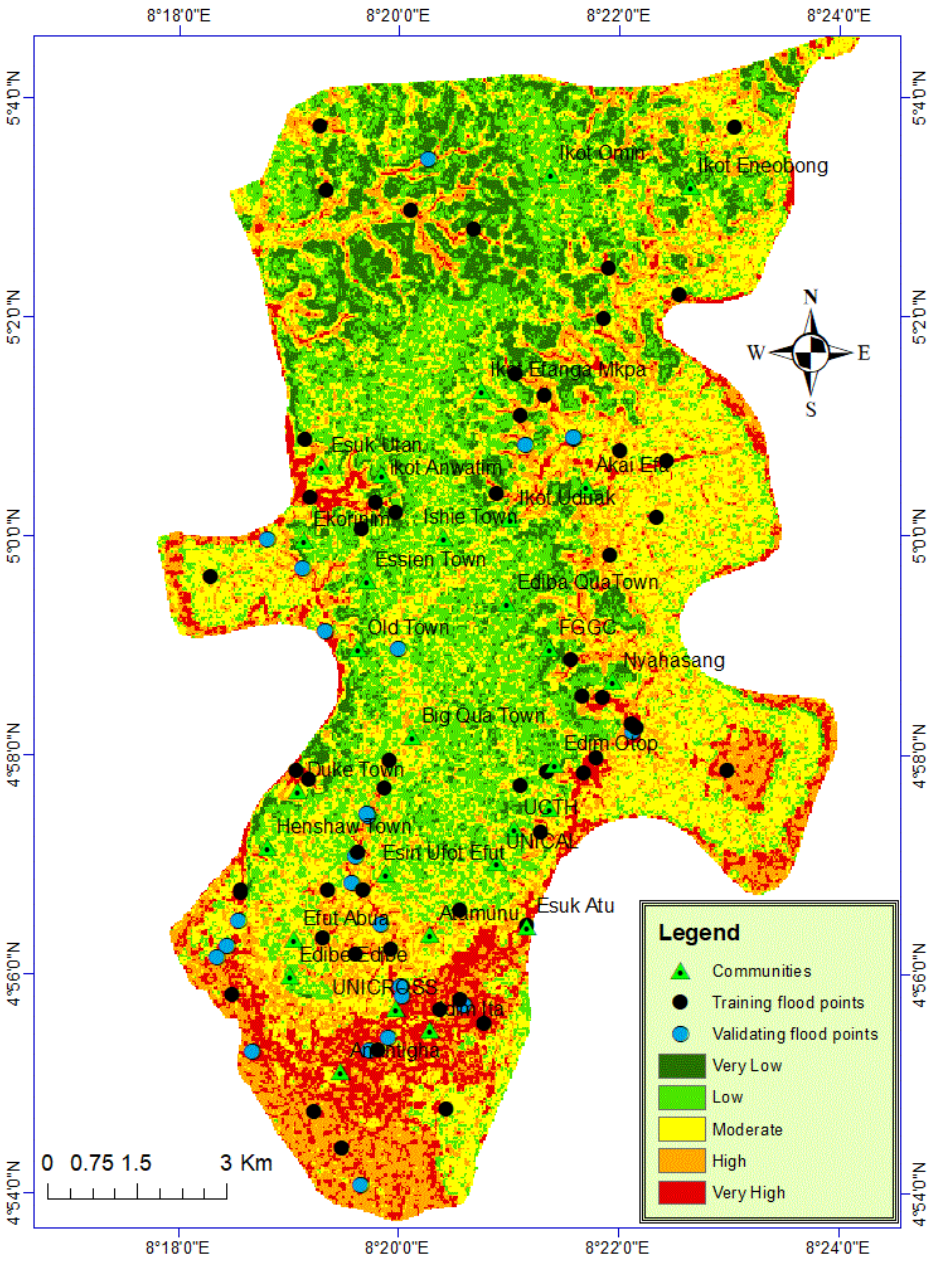

Figure 6 Flood susceptibility map of Calabar.

3) Analysis of flood susceptibility model

The FSIas obtained in this study is given as Eq. 12.

Eq. 12 consists of the summation of 8 flood conditioning factors (land cover, NDVI, slope, aspect, TPI, TWI, curvature and elevation). The calculated FSI values ranged from 99.26 – 716.01 and was classified using the Natural breaks (Jenks) method into five classes. This resulted in the FSI map in Figure 6. The 5 classes of the flood susceptibility map were interpreted as follows: very low (FSI: 99.26–226.15), low (FSI: 226.15–348.38), moderate (FSI: 348.38–428.20), high (FSI: 428.20–517.69) and very high (FSI:517.69–716.01). Table 2 shows the percentage areal coverage of the various classes of the flood susceptibility map.

Table 2 Flood susceptibility coverage of the various zones

Class	Area (km^2)	Area (%)	Susceptibility level
1	14.49	10.59	Very Low
2	38.70	28.28	Low
3	43.50	31.79	Moderate
4	27.33	19.97	High
5	12.82	9.37	Very High

4) Model validation

One important aspect of hazard susceptibility mapping is the validation of the potentiality of the occurrence of the hazard. The area under the curve (AUC) is a common, all-encompassing technique of assessing accurateness of the forecast and success rates [41, 56], that was adopted in this study. It was executed by comparing defined flood data with the likelihood map of acquired flooding. The techniques involved splitting the probability map into categories of equal-area, with the performance and prediction curves determining the category of each probability. In adopting this approach for flood susceptibility assessment, the x-axis of the AUC represents specificity (the probability of misprediction of the non-flood points), while the y-axis highlights sensitivity (the success rate of the flood point). The prediction accuracy of the model is determined by the size of the area enclosed by the curve and the abscissa. If the sensitivity and specificity of the model is high, the Receiver operator curve (ROC) will hug the top left corner of the plot. This means that, the closer the curve is to the upper left corner of the plot, the higher the accuracy of the model. AUC values range from 0 to 1, where the value of 0 indicates a perfectly inaccurate test and the value of 1 reveals a perfect test. Generally, an AUC of 0.5 suggests no discrimination in the test, 0.7 to 0.8 is considered acceptable, 0.8 to 0.9 is taken as excellent, and greater than 0.9 is said outstanding. In the present study, the AUC was found to be 0.7481 or 74.81 percent (Figure 7). Hence, the result of the test was considered acceptable for flood susceptibility prediction in the study area.

$$FSI = Landcover * 1.48 + NDVI * 1.52 + Slope * 1.09 + Aspect * 1.21 + TPI * 2.89 - TWI * 1 + Curvature * 1.43 + Elevation * 2.56 \quad \text{(Eq. 12)}$$

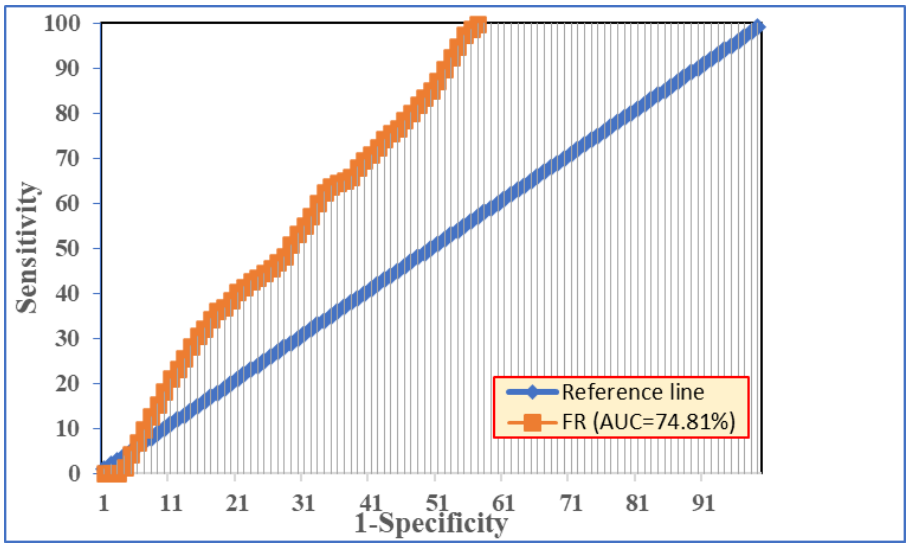

Figure 7 Receiver operator curve (ROC).

Discussion

The four main objectives that were set for this study were to: 1. examine the nature of the various flood conditioning factors in Calabar City; 2. investigate the influence of the various conditioning factors on flood susceptibility of Calabar City; 3. develop a robust flood susceptibility model for the study area; 4. validate the developed model in 3 above. Eight flood conditioning factors (elevation, slope, aspect, curvature, TPI, TWI, land cover and NDVI) were adopted in this study. These factors revealed different levels of relationships with flood occurrence in the area. The discussion follows the level of contribution of each of the factors based on the prediction rate.

TPI with a prediction rate of 2.89 made the highest contributions to the explanation of flooding in the study area. The results further reveal that over 90 percent of flooding occurred where TPI values are negative. It has been shown that areas with negative TPI pose higher risk to flooding than those with positive TPI values [57]. Hence, areas with negative TPI are susceptible to flooding in Calabar City.

Elevation in the present study has a prediction rate of 2.56 and was rated as the second most significant contributing factor to flooding in the study area. The result shows that there is an inverse relationship between elevation and flooding in the study area. The importance of elevation in hydrological studies cannot be misplaced. It has been established that elevation sets environmental control and provides the basis for spatial variation in hydrological conditions in a particular region [40]. It is also considered as the most important factor affecting flood modelling [54, 58]. As a major variable in topography, elevation has been found to have significant impact in flood incidence since water often flows from higher elevations to lower land areas [59, 23]. There is a low probability of flooding in higher elevations and a high likelihood in the lowland areas [46]. Hence, elevation was found to play a significant role in flooding in the study area because places with lower elevation classes experienced more flooding than those in higher classes.

The third most significant flood conditioning factor in the study is the NDVI, with a prediction rate of 1.82. Negative NDVI values are often an indication of water while positive values reflect vegetation. Hence, there is a strong association between negative NDVI and flooding. Invariably, higher NDVI values suggest a lesser flood risk and vice versa [52]. Again, the results from this study showed that over 90 percent of flood points occurred where NDVI ranged between 0.02 and 0.15, representing bare surfaces, shrubs and/or crops [55]. Areas of bare surfaces (including build-up), tend to reduce infiltration, hence increasing runoff that leads to flooding. In the same vein, land cover distribution was the fourth most significant contributor to flood susceptibility in the study area with a prediction rate of 1.48. The 6 land cover classes which were extracted in this study included undisturbed forest (23.56 percent), disturbed forest (8.88 percent), grassland/open parks (0.02 percent), cropland (28.04 percent), built-up (39.01 percent) and water body (0.49 percent). Here, over 70 percent of flooding occurred on built-up and cropland areas. Built-up presents bare surfaces and reduces infiltration of water into the soil. This enhances runoff which leads to flooding. This confirms the assertion that unprotected areas are more susceptible and vulnerable to flooding than protected areas [23].

Curvature is a second derivative of topography and also has a significant role in water movement on the surface of the earth. From the results (Table 1), curvature made the fifth most significant contribution to flood susceptibility in the study area with a prediction rate of 1.43. Table 1 again showed that approximately 76 percent of previous floods occurred on slopes with flat or convex forms. Hence, flat and convex surface plays significant roles in flooding in the study area. This finding is in agreement with the fact that runoff convergence operation is related to the negative value regions [60] and such areas have been shown to be highly susceptible to flooding [22].

Aspect has proved to be a very useful indicator of hydrologic conditions since it is linked to topographic trends and soil moisture patterns [46]. Aspect is one of the first derivatives of elevation with significant impact on hydrologic processes including frontal precipitation direction and evapotranspiration [41]. Aspect was the sixth most significant conditioning factor to flood in this study, with a prediction rate of 1.21. The results of the present study revealed higher FR for high aspect ranges. For instance, aspect range of 141-212 and 212-282 has FR > 1. Similarly, slope as one of the first derivatives of elevation has significant controls on the occurrence of flooding. Slope controls the speed of the flowing water [61]. The lower the angle of slope, the higher the possibility of water stagnation, the higher the rate of infiltration and the lower the speed of water flow. Studies have shown that flooding and flood events are more likely to occur with low slope gradient. Higher gradients reduce penetration while increasing surface runoff and vice versa. Hence, where slope gradient is low, a large amount of water becomes inactive, resulting in flooding [23]. In the present study, slope had a prediction rate of 1.09, with about 79 percent of historical floods occurring where slope gradient is < 2.36º (Table 1). These findings are similar to those of other studies [23]. Hence slope in the study area play significant role in flooding.

Another topographic index that was developed in the present study is TWI which had a prediction rate of 1. Generally, topographic indices have been found to play significant roles in the occurrence of most hydrologic hazards [41]. Topography therefore plays a very significant role in occurrence of flooding in the study area, with two major anticlinal structures with a syncline serving as the major topographic features that control movement of surface water in the city [4].

The flood susceptibility map (Figure 6) reveals that about 9 and 20 percent of the study area falls under very high and high susceptibility levels respectively. These account for about 30 percent of the study area covering about 40.15 km^2 of the total surface of the study area. If we include the portion with the moderate susceptibility level, this will account for about for about 60 percent of the entire area. The most affected parts of the city are those in the southern part (Calabar South), the north central portion, the eastern and western fringes (Figure 6). This is because elevation in the southern part of the study area is generally low when compared with the northern portion. Also, the study area slopes towards the southern part of the city and the rivers on the eastern and western flanks of the city (Figure 1). These areas fall with the high and very high flood susceptibility classes in the study area. Only about 40 percent of the entire area falls under low and very low flood risk zone (Table 2).

The FR model used in this study has shown that elevation, slope gradient, aspect, curvature, TWI, TPI, NDVI and land cover type were able to predict flood susceptibility in the study area (Eq. 13). For purposes of clarity, low elevation, low slope gradient, high aspect range, flat surfaces, low NDVI and presence of cropland and build-up areas were responsible for flooding in the study area. In terms of success rate and prediction accuracy, the FR model's performance returned an AUC of 0.7481 per cent (Figure 7), indicating an acceptable predicting ability [41, 56, 59].

Conclusion

The frequency ratio model was used to investigate the flood susceptibility of Calabar City in Cross River State of Nigeria. Eight flood conditioning factors (elevation, slope, aspect, curvature, TWI, TPI, land cover and NDVI were identified and included in the FR model. It was concluded that Low TPI, low elevation, low slope gradient, high aspect range, flat surfaces, low NDVI and presence of cropland and build-up areas were responsible for flooding in the study area. The southern part of the study area and parts of the fringes are more susceptible to flooding that the northern and central part, except for areas that lies within the major geosyncline in the study area. The ROC that was used to assess and measure the significance of the current FR model for vulnerability mapping revealed an AUC of 0.7481 which was considered acceptable for modelling flood susceptibility of the city. The resultant flood susceptibility map has implications of land development in the study area and will assist the government officers, planners, and policy makers in implementing appropriate administrative plans to mitigate risk due to flash floods in the study area. Hence, geospatial scientists and allied professionals, particularly those in town planning office in Calabar should make the output of this work their veritable companion in suggesting and or giving approval for land development to avoid flood impacts in the future. However, the findings of this study are limited to only land surface information that were included in the FR model. With recent interest in flood management, particularly in Nigeria, flood susceptibility mapping should be extended to other cities and river basins across the country to safeguard lives and property. Moreover, machine learning approaches, known for higher prediction accuracies, could be adopted in future research in the study area and other similar locations.

References

[1] Tehrany, M.S., Pradhan, B., Juber, M.N. Flood susceptibility analysis and its verifcation using a novel ensemble support vector machine and frequency ratio method. Stochastic Environmental Research and Risk Assessment., 2015.

[2] Pradhan, B. Flood susceptible mapping and risk area delineation using logistic regression, GIS and remote sensing. Journal of Spatial Hydrology, 2010, 9, 1.

[3] Wang, Y., Fang, Z., Hong, H., Peng, L. Flood susceptibility mapping using convolutional neural network frameworks. Journal of Hydrology, 2020, 582, 124482.

[4] Eze, E.B. Topography and urban expansion as twin factors of street flooding in Calabar Municipality, Cross River State. *In*: Bisong, F.E. Geography and the millennium development goals: Translating vision into Reality in Nigeria. Calabar: Index Book Publishers Limited, 2008, 415–422.

[5] Eze, E.B., Efiong, J. Morphometric parameters of the Calabar river basin: implication for hydrologic processes. Journal of Geography and Geology, 2010, 2(1), 18–26.

[6] Efiong, J., Uzoezie A.D. Increased paved surfaces as major factor of urban flooding in humid tropics: An example from Calabar, Cross River State,

Nigeria. World Environment Journal, 2017, 1(1), 45–57.

[7] Njoku, C.G., Efiong, J., Ayara, N.N. A geospatial expose of flood risk and vulnerable areas in Nigeria. International Journal of Applied Geopstial Research, 2020, 11(3), 87–110.

[8] WHO. Disaster data-key trends and statistics in world disasters report. Geneva, Switzerland: WHO, 2003.

[9] Efiong, J. Effect of landuse on water discharge in humid regions: an example from Southeastern Nigeria. Global Journal of Social Sciences, 2011, 10, 53–61

[10] Ekpoh, I.J. Recent severe flooding in Calabar, Nigeria: Causes, consequences and possible remedies. International Journal of Sciences, 2014, 3(1), 102–104.

[11] Efiong, J., Hogan, I.S. Mapping flood risk zones in the Cross-River basin using remote sensing and geographical information systems. Proceedings of the 8th International Conference of Nigeria Association of Hydrological Sciences (NAHS), 2017, 161–166.

[12] Efiong, J., Ushie, J.O. Projected impact of sea level rise on Nigeria's coastal city of Calabar in Cross River State. International Journal of Environment and Climate Change, 2019, 9(10), 535–548.

[13] Umaru, E.T., Adedokun, A. Geospatial analysis of flood risk and vulnerability assessment along River Benue Basin of Kogi State. Journal of Geographic Information System, 2020, 12, 1–1.

[14] Maclean, R. Nigeria floods kill hundreds and displace over a million. The New York Times. 2022. [Online] Available from: https://www.nytimes.com/2022/10/17/world/africa/nigeria-floods.html [Accessed 20 January 2023].

[15] Wanjohi, K. Nigeria floods 80 times more likely with climate change'. 2020. AP NEWS. [Online] Available from: https://apnews.com/article/floods-science-africa-nigeria-climate-and-environment-7972ff1cba1134cc80219acff1a51d42 [Accessed 20 January 2023].

[16] Bayo, W. Why a dam in Cameroon causes devastating floods in Nigeria every year [Pulse Explainer]. Pulse Nigeria, 2022. [Online] Available from: https://www.pulse.ng/news/local/why-a-dam-in-cameroon-causes-devastating-floods-in-nigeria-every-year/py1twye

[17] Punch Newpaper, How Calabar flood targets 'Target Street' to flush out residents, 2017. [Online] Available from: https://punchng.com/how-calabar-flood-targets-target-street-to-flush-out-residents/

[18] Amangabara, G.T., Obenade, M. Flood vulnerability assessment of Niger Delta States relative to 2012 flood disaster in Nigeria. American Journal of Environmental Protection, 2015, 3, 76–83.

[19] Afolabi, O.O., Emelu, V.O., Wali, E., Orji, M.C., Bosco-Abiahu, L.C., Yemi-Jonathan, O.I.T., …, Asomaku, S.O. Geospatial analysis of flood vulnerability levels based on physical characteristics and resilience capacity of Peri-Urban Settlements in Nigeria. Journal of Geoscience and Environment Protection, 2022, 10, 267–288.

[20] Sahana, M., Rehman, S., Sajjad, H., Hong, H. Exploring effectiveness of frequency ratio and support vector machine models in storm surge flood susceptibility assessment: A study of Sundarban Biosphere Reserve, India. Catena, 2020, 189, 104450.

[21] Ogunwumi, T.S., Waziri, E.S., Udoh, J.C. Geospatial mapping of flood hazard using multi-criteria approach in Fufore Local Government Area, North Eastern Nigeria. Journal of Basic and Applied Research International, 2021, 27 (3), 13–26.

[22] Islam, A.R.M.T., Salukdar, S., Mahato, S., Kundu, S., Eibek, K.U., Pham, Q.B., …, Linh, N.T.T. Flood susceptibility modelling using advanced ensemble machine learning models. Geoscience Frontiers, 2021, 12, 101075.

[23] Munir, A., Ghufran, M.A., Ali, S.M., Majeed, A., Batool, A., Khan. M.B.A.S., Abbasi, G.H. Flood susceptibility assessment using frequency ratio modelling approach in Northern Sindh and Southern Punjab, Pakistan. Polish Journal of Environmental Studies, 2022, 31(4) 3249–3261.

[24] Megahed, H.A., Abdo, A.M., AbdelRahman, M.A.E., Scopa, A., Hegazy, M.N. Frequency ratio model as tools for flood susceptibility mapping in urbanized areas: A case study from Egypt. Applied Sciences, 2023, 13, 9445.

[25] Ozay, B., Orhan, O. Flood susceptibility mapping by best-worst and logistic regression methods in Mersin, Turkey. Environmental Science and Pollution Research, 2023, 30(15), 45151–45170.

[26] Waiyasusri, K. Wetchayont, P., Tananonchai, A., Dolreucha, S. Flood susceptibility mapping using logistic regression analysis in Lam Khan Chu Watershed, Chaiyaphum Province, Thailand, 2023, 16.

[27] Tehrany, M.S., Pradhan, B., Jebur, M.N. Spatial prediction of flood susceptible areas using rule based decision tree (DT) and a novel ensemble

bivariate and multivariate statistical models in GIS. Journal of Hydrology, 2013, 504, 69–79.

[28] Lyu, H., Yin, Z. Flood susceptibility prediction using tree-based machine learning models in the GBA, Sustainable Cities and Society, 2023, 97, 104744.

[29] Ren, H., Pang, B., Bai, P., Zhao, G., Liu, S., Liu, Y., Li, M. Flood susceptibility assessment with random sampling strategy in ensemble learning (RF and XGBoost). Remote Sensing, 2024, 16, 320.

[30] Abedi, R., Costache, R., Shafizadeh-Moghadam, H., Pham, Q.B. Flash-Flood susceptibility mapping based on XGBoost, random forest and boosted regression trees. Geocarto International. 2022, 37, 5479–5496.

[31] Tehrany, M.S., Pradhan, B., Mansor, S., Ahmad, N. Flood susceptibility assessment using GIS-based support vector machine model with different kernel types. Catena, 2015, 125, 91–101.

[32] Salvati, A., Nia, A.M., Salajegheh, A., Ghaderi, K., Asl, D.T., Al-Ansari, N., …, Clague, J.J. Flood susceptibility mapping using support vector regression and hyper-parameter optimization. Journal of Flood Risk Management, 2023, 16(4), e12920.

[33] Rahman, M., Ningsheng, C., Islam, M.M., Dewan, A., Iqbal, J., Washakh, R.M.A., Shufeng, T. Flood susceptibility assessment in Bangladesh using machine learning and multi-criteria decision analysis. Environmental Earth Sciences, 2019, 3 (3), 585–601.

[34] Kia, M.B., Pirasteh, S., Pradhan, B., Mahmud, A.R., Sulaiman, W.N.A., Moradi, A. An artificial neural network model for flood simulation using GIS: Johor River Basin, Malaysia. Environmental Earth Sciences, 2012, 67 (1), 251–264.

[35] Haq, M., Akhtar, M., Muhammad, S., Paras, S., Rahmatullah, J. Techniques of remote sensing and GIS for flood monitoring and damage assessment: A case study of Sindh Province, Pakistan. Egyptian Journal of Remote Sensing and Space Science, 2012, 15(2), 135.

[36] Seejata, K., Yodying, A., Chatsudarat, S., Chidburee, P., Mahavik, N., Kongmuang, C., Tantanee, S. Assessment of flood hazard using geospatial data and frequency ratio model in Sukhothai Province, Thailand, Korea: Daejeon Convention Center(DCC), Daejeon, Korea, The 40th Asian Conference on Remote Sensing (ACRS 2019) October 14–18, 2019.

[37] Sarkar, D., Mondal, P. Flood vulnerability mapping using frequency ratio (FR) model: A case study on Kulik river basin, Indo Bangladesh Barind region. Applied Water Science, 2020, 10, 17.

[38] Samanta, S., Pal, D.K., Palsamanta, B. Flood susceptibility analysis through remote sensing, GIS and frequency ratio model. Applied Water Science, 2018.

[39] Tehrany, M.S., Shabani, F., Jebur, M.N., Hong, H., Chen, W., Xie, X. GIS-based spatial prediction of food prone areas using standalone frequency ratio, logistic regression, weight of evidence and their ensemble techniques. Geomatatics Natural Hazards and Risk, 2017, 8(2), 1538–1561.

[40] Pawar, U., Suppawimut, W., Muttil, N., Rathnayake, U. A GIS-based comparative analysis of frequency ratio and statistical index models for flood susceptibility mapping in the Upper Krishna Basin, India. Water, 2022, 14, 3771.

[41] Efiong, J., Eni, D.I., Obiefuna, J.N., Etu, S.J., Geospatial modelling of landslide susceptibility in Cross River State of Nigeria. Scientific African, 2021, 14, e01032.

[42] Rahmati, O., Pourghasemi, H.R., Zeinivand, H. Flood susceptibility mapping using frequency ratio and weights-of-evidence models in the Golastan Province, Iran. Geocarto International, 2016, 31(1), 42–70.

[43] Sinha, R., Bapalu, G.V., Singh, L.K., Rath, B. Flood risk assessment in the Kosi River basin, North Bihar using multi-parametric approach of analytical hierarchy process (AHP). Journal of the Indian Society of Remote Sensing, 2008, 36, 335–349.

[44] Chen, Y.-R., Yeh, C.-H., Yu, B. Integrated application of the analytic hierarchy process and the geographic information system for flood risk assessment and flood plain management in Taiwan. Natural Hazard, 2011, 59(3), 1261–1276.

[45] Rahman, M., Ningsheng, C., Islam, M.M., Dewan, A., Iqbal, J., Washakh, R.M.A., Shufeng, T. Flood susceptibility assessment in Bangladesh using machine learning and multi-criteria decision analysis. Earth Systems and Environment, 2019, 3(3), 585–601.

[46] Das, S. Geospatial mapping of flood susceptibility and hydro-geomorphic response to the floods in Ulhas Basin, India. Remote Sensing Applications: Society and Environment, 2019, 14, 60–74.

[47] Das, S. Flood susceptibility mapping of the Western Ghat coastal belt using multi-source geospatial data and analytical hierarchy process (AHP). Remote Sensing Applications: Society and Environment, 2020, 20, 100379.

[48] Cross River Basin Development Authority. Inventory of natural site conditions – map, 1982.

[49] Nyong, E.E. Cretaceous sediments in Calabar Flank. *In*: Ekwueme, B.N., Nyong, E.E., Petters, S.W. Geological excursion guidebook to Oban Massif, Calabar Flank and Mamfe Embayment, Southeastern Nigeria. Calabar: Dec. Ford Publishers, 1995, 17–26.

[50] https://www.usgs.gov/media/images/shuttle-radar-topography-mission-srtm-1-arc-second-0

[51] https://earthexplorer.usgs.gov/LC08_188056_20220205_20220212_02-T1

[52] Longley, P.A., Goodchild, M., Maguire, D.J., Rhind, D.W. Geographic information systems and science. 3rd Edition. London: John Wiley & Sons, 2011.

[53] Torcivia, C.E.G., Lypez, N.N.R. Preliminary Morphometric Analysis: Rho Talacasto Basin, Central Precordillera of San Juan, Argentina. Advances in Geomorphology and Quaternary Studies in Argentina. Springer, Cham, 2020,158–168.

[54] Bui, D.T., Hoang, N.D., Martinez-Alvarez, F., Ngo, P.T.T., Hoa, P.V., Pham, T.D., Costache, R. A novel deep learning neural network approach for predicting flash flood susceptibility: A case study at a high frequency tropical storm area. Science of the Total Environment, 2020, 701, 134413.

[55] Kshetri, T.B. NDVI, NDBI and NDWI calculation using LANDSAT 7 and 8. Geomatics for Sustainable Development, 2018, 2, 32–33.

[56] Egan, J.P. Signal detection theory and ROC analysis. New York: Academic, 1975, 266–268.

[57] Bashir, B. Morphometric parameters and geo-spatial analysis for flash flood susceptibility assessment: A case study of Jeddah City along the Red Sea Coast, Saudi Arabia. Water, 2023, 1, 870.

[58] Dodangeh, E., Choubin, B., Eigdir, A.N., Nabipour, N., Panahi, M., Shamshirband, S., Mosavi, A. Integrated machine learning methods with resampling algorithms for flood susceptibility prediction. Science of the Total Environment, 2020, 705, 135983.

[59] Sahana, M., Patel, P.P. A comparison of frequency ratio and fuzzy logic models for flood susceptibility assessment of the lower Kosi River Basin in India. Environmental Earth Sciences, 2019, 78(10), 1.

[60] Costache, R., Bui, D.T. Identification of areas prone to flash-flood phenomena using multiple-criteria decision-making, bivariate statistics, machine learning and the ensembles. Science of the Total Environment, 2020, 136492.

[61] Stevaux, J.C., de Azevedo Macedo, H., Assine, M.L., Silva, A. Changing fluvial styles and backwater flooding along the upper Paraguay River plains in the Brazilian Pantanal wetland. Geomorphology, 2020, 350, 106906.